Journal of Medicinal Chemistry Article

J. Med. Chem. **XXXX,** *XXX,* 000–000 **A**
DOI: 10.1021/jm9016637

New Angiopep-Modified Doxorubicin (ANG1007) and Etoposide (ANG1009) Chemotherapeutics With Increased Brain Penetration

Christian Ché,[†] Gaoqiang Yang,[†] Carine Thiot,[†] Marie-Claude Lacoste,[†] Jean-Christophe Currie,[‡] Michel Demeule,*[,†] Anthony Régina,[†] Richard Béliveau,[‡] and Jean-Paul Castaigne[†]

[†]*Angiochem, 201 President Kennedy Avenue (PK-R220), Montreal, Québec, Canada H2X 3Y7, and* [‡]*Laboratoire de Médecine Moléculaire, Université du Québec à Montréal, Montréal, Québec, Canada*

Received November 10, 2009

This report describes the synthesis and preliminary biological characterization of **2** (ANG1007) and **3** (ANG1009), two new chemical entities under development for the treatment of primary and secondary brain cancers. **2** consists of three doxorubicin molecules conjugated to Angiopep-2, a 19-mer peptide that crosses the blood−brain barrier (BBB) by an LRP-1 receptor-mediated transcytosis mechanism. **3** has a similar structure, with the exception that three etoposide moieties are conjugated to Angiopep-2. Both agents killed cancer cell lines in vitro with similar IC_{50} values and with apparently similar cytotoxic mechanisms as unconjugated doxorubicin and etoposide. **2** and **3** exhibited dramatically higher BBB influx rate constants than unconjugated doxorubicin and etoposide and pooled within brain parenchymal tissue. Passage through the BBB was similar in *Mdr1a* (−/−) and wild type mice. These results provide further evidence of the potential of this drug development platform in the isolation of novel therapeutics with increased brain penetration.

Introduction

Doxorubicin and etoposide exhibit excellent therapeutic activity against a variety of solid tumors.[1−4] Doxorubicin, a cytotoxic anthracycline antibiotic that intercalates into DNA, is thought to promote cytotoxicity by inhibiting DNA and RNA polymerases and by interacting with topoisomerase II to form DNA-cleavable complexes.[5] Etoposide, a semisynthetic derivative of podophyllotoxin used for different malignancies and as first line treatment in small cell lung cancer,[6] is thought to promote cytotoxicity by disrupting cell cycle progression, presumably by promoting DNA strand breaks in combination with DNA topoisomerase II.[7]

Chemotherapy for malignant brain tumors often has limited efficacy, largely due to restricted blood−brain barrier (BBB[a]) permeability for chemotherapeutic drugs.[8] Intercellular tight junctions between capillary endothelial cells, a continuous (i.e., nonfenestrated) capillary endothelium, multiple intracellular efflux pumps with broad substrate specificity, and an array of intracellular and extracellular degradative/metabolic enzymes all combine to produce the restrictive diffusion barrier characterizing the BBB.[9−12] Penetration of both doxorubicin and etoposide into brain tissue is dramatically inhibited by the BBB.[13,14]

We have developed a novel drug-development technology called the engineered peptide compound (EPiC) platform that exploits the endogenous LRP-1 receptor-mediated transcytosis system. This platform is based on a proprietary 19-amino-acid sequence, called Angiopep-2, that crosses the BBB by an LRP-1 mediated mechanism. **1** (ANG1005),[13,15] a new chemical entity (NCE) under development for the treatment of primary and secondary brain cancers, is the first agent to reach clinical trials based on this platform.[16] **1** (Figure 1) is composed of one Angiopep-2 peptide conjugated to three molecules of paclitaxel, a broad-spectrum antitumor agent that inhibits reorganization of microtubules during interphase and mitosis. In mice, **1** inhibited growth of orthotopic human glioblastoma (U87 MG) brain tumors more potently than paclitaxel alone and significantly increased animal survival rates.[16] In phase I clinical trials in humans, **1** reached therapeutic concentrations in brain tumors and produced significant antitumor responses in patients with primary gliomas or secondary brain metastases who had failed prior standard therapy.[17,18] The present study describes the synthesis and preliminary biological characterization of two new Angiopep-modified doxorubicin and etoposide derivatives with increased brain penetration.

Chemistry

Synthesis. The first derivative **2** consists of three molecules of doxorubicin conjugated via a cleavable ester bond to one Angiopep-2 peptide (Figure 1). For its synthesis (Scheme 1), the primary amine in the sugar of doxorubicin was first protected by an Fmoc group to provide intermediate **4** in

*To whom correspondence should be addressed. Phone: 514-987-3000 ext. 4087/6697. Fax: 514-987-0246; E-mail: mdemeule@angiochem.com.

[a] Abbreviations: LRP1, low-density lipoprotein receptor-related protein; pAb, polyclonal antibody; PBS, phosphate-buffered saline; BBB, blood−brain barrier; DMSO, dimethylsulfoxide; UPLC, ultra performance liquid chromatography; FA, formic acid; DIEA, *N*,*N*-diisopropylethylamine; FmocOSu, *N*-(9-fluorenylmethoxycarbonyloxy) succinimide; DMF, *N*,*N*-dimethylformamide; TFA, trifluoroacetic acid; DCM, dichloromethane; TBTU, *O*-(benzotriazol-1-yl)-*N*,*N*,*N*′,*N*′-tetramethyluronium tetrafluoroborate; RPC, reverse phase chromatography; DMAP, 4-dimethylaminopyridine.

© XXXX American Chemical Society

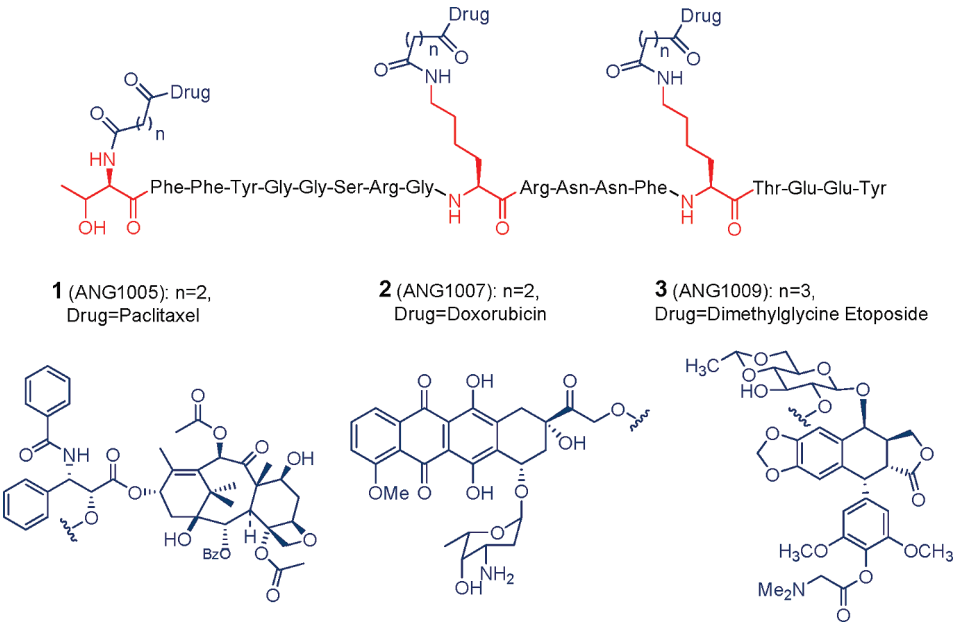

Figure 1. Chemical structure of **1**, **2**, and **3**. **1** , **2**, and **3** are each composed of three molecules of paclitaxel, doxorubicin, and etoposide, respectively, linked by cleavable ester to the Angiopep-2 peptide.

Scheme 1. Synthesis of **2**

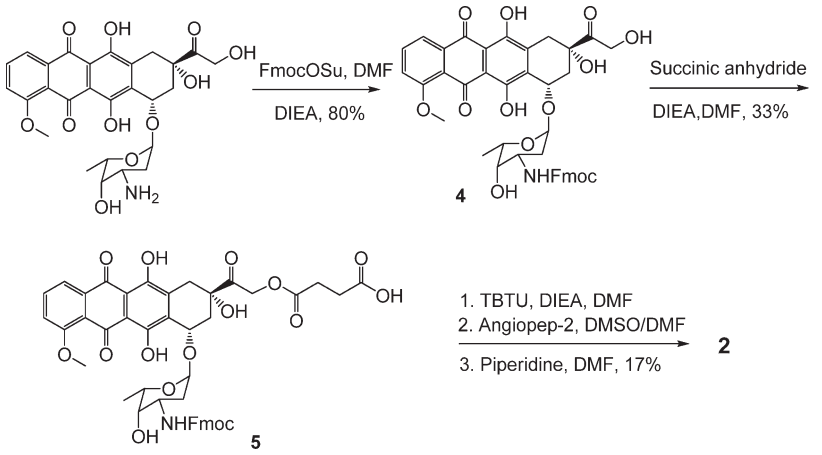

Scheme 2. Synthesis of **3**

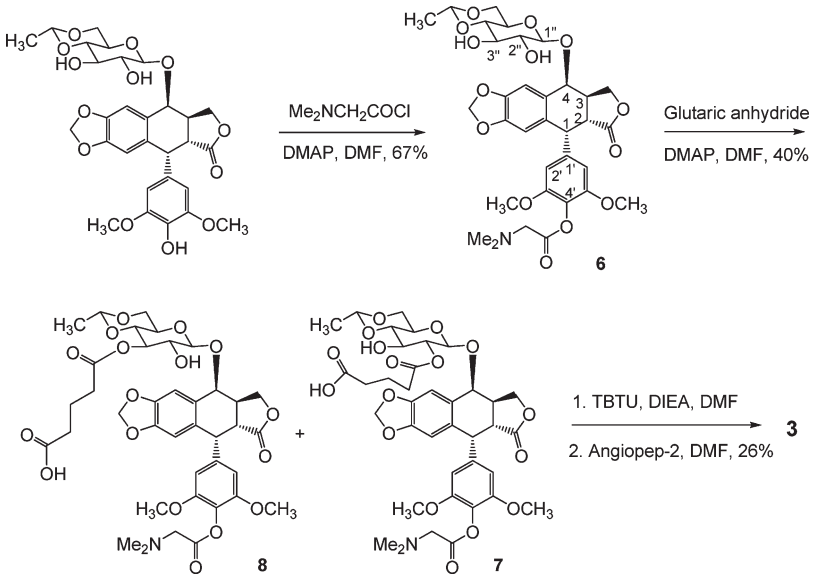

good yield (80%), which was then reacted with succinic anhydride to afford, primarily, the key acid **5**. Some bis-acylated side-products, via the two hydroxyls, were also formed (< 15%) and removed by SiO_2 purification. The free acid **5** was activated by TBTU prior to in situ conjugation with Angiopep-2. Under standard Fmoc deprotection conditions, the desired product **2** was obtained in 17% yield after purification on an AKTAexplorer system (GE Healthcare Life Sciences, Baie d'Urfe, Québec, Canada; see Experimental Section).

The second derivative **3** consists of three molecules of etoposide conjugated via a cleavable ester bond to the Angiopep-2 peptide (Figure 1). For the synthesis of **3** (Scheme 2), a dimethyl amino acetyl group was first introduced by acetylation at the 4′ position of the phenol of etoposide to generate intermediate **6** in 67% yield, which was then reacted with glutaric anhydride in the presence of DMAP to produce, primarily, semiglutarate **7** at the 2″ position in 40% yield. Some regioisomer **8** at the 3″ position was also isolated in 5% yield. The assignment of regioisomers **7** and **8** was performed by proton chemical shifts (Table 1)[19] and confirmed by correlation spectroscopy (COSY) (data not shown). Regioisomer **7** was conjugated in situ with Angiopep-2 as previously described to provide **3** in 26% yield.

3 was soluble in dextrose 5% in water (D5W) up to 20 mg/mL. Similarly, the HCl salt of **2** could be dissolved at the same concentration in D5W. The high solubility of **2** and **3** facilitated their in vitro and in vivo studies.

Analysis of End-Products. HPLC profiles of the final synthetic products exhibited single peaks with retention times for **2** (4.8 min) and **3** (5.4 min) that were distinct from unconjugated Angiopep-2 (4.2 min) (Figure 2). The masses of the HPLC-purified final products, as determined by mass spectrometry, were consistent in each case with three drug moieties conjugated to a single Angiopep-2 peptide. Thus, the observed mass of purified **2** (LC-HRMS, ESI, *m*/*z* 2089.9674 [M + 2], 1393.2419 [M + 3], and 1045.4395 [M + 4]) was consistent with the calculated mass of $C_{197}H_{242}N_{32}O_{70}$ (4177.6428) (Figure 3A). Similarly, the observed mass of purified **3** (*m*/*z* 2305.9327 [M + 2], 1537.6443 [M + 3], 1153.7463 [M + 4], and 922.7970 [M + 5]) was consistent with the calculated mass of $C_{218}H_{281}N_{32}O_{79}$ (4610.8955) (Figure 3B). **2** and **3** with purities >95% were used in all subsequent biological assays.

Table 1. Proton Chemical Shifts at the 2″ and 3″ Positions for Etoposide, Compounds **6**, **7**, and **8**

	δ (ppm) in CD_3OD			
proton	etoposide[19]	**6**	**7**	**8**
2″	3.25	3.32	4.74	3.44
3″	3.53	3.52	3.78	4.76

Results and Discussion

In Vitro Cytotoxicity. The in vitro cytotoxic activities of **2** and **3** were evaluated using a thymidine incorporation assay. To do so, human tumor cell lines were incubated for 48 h in the presence of increasing concentrations of **2**, **3**, doxorubicin, or etoposide. After aspirating off the old media, cells were pulse-labeled for 2 h in fresh media containing [^{3}H]-thymidine. Uptake of tritium was evaluated in a β counter, and the drug concentrations required to inhibit cell proliferation by 50% (IC_{50}) were calculated. Results from these experiments showed that, in general, **2** and **3** had cytotoxic activities that were comparable to their parental drugs (doxorubicin and etoposide) in U87 MG glioblastoma, SK-Hep-1 hepatocarcinoma, and NCI-H460 lung carcinoma cell lines (Table 2), albeit **3** appeared to be somewhat less potent than etoposide in glioblastoma and lung carcinoma cells.

For **2** and **3**, as well as the earlier agent **1**, conjugation of the individual anticancer drugs to Angiopep-2 was achieved via a cleavable ester bond. When doxorubicin was conjugated to Angiopep-2 via a noncleavable linker, however, the Angiopep-2-doxorubicin conjugate lost its antiproliferative activity, indicating that doxorubicin needed to be released from the peptide to be active in cancer cells (data not shown). To evaluate their in vitro half-lives, a release study was performed on **2** and **3** by incubating the drugs in human serum for 0−4 h and quantifying the release of doxorubicin

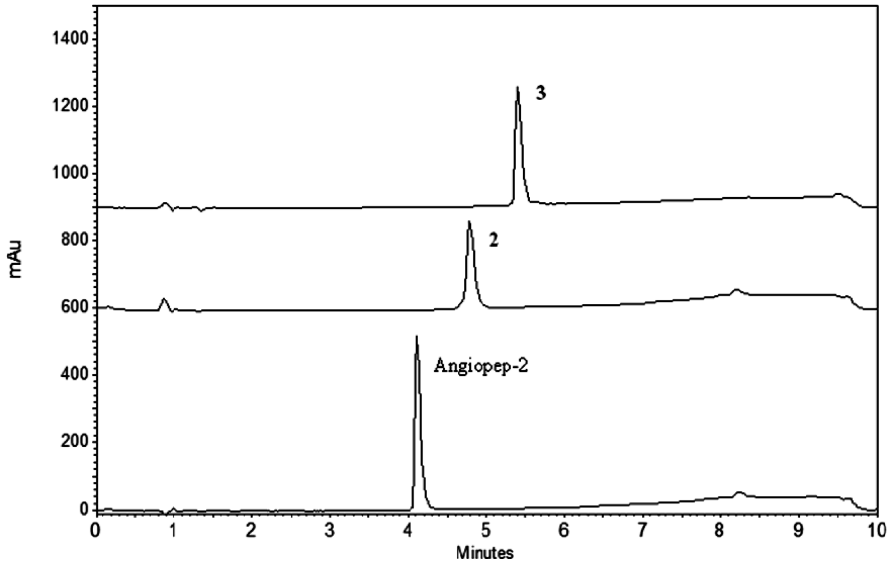

Figure 2. HPLC analysis of Angiopep-2, **2**, and **3**. Representative chromatograms obtained for Angiopep-2, **2**, and **3** showing three distinct retention times.

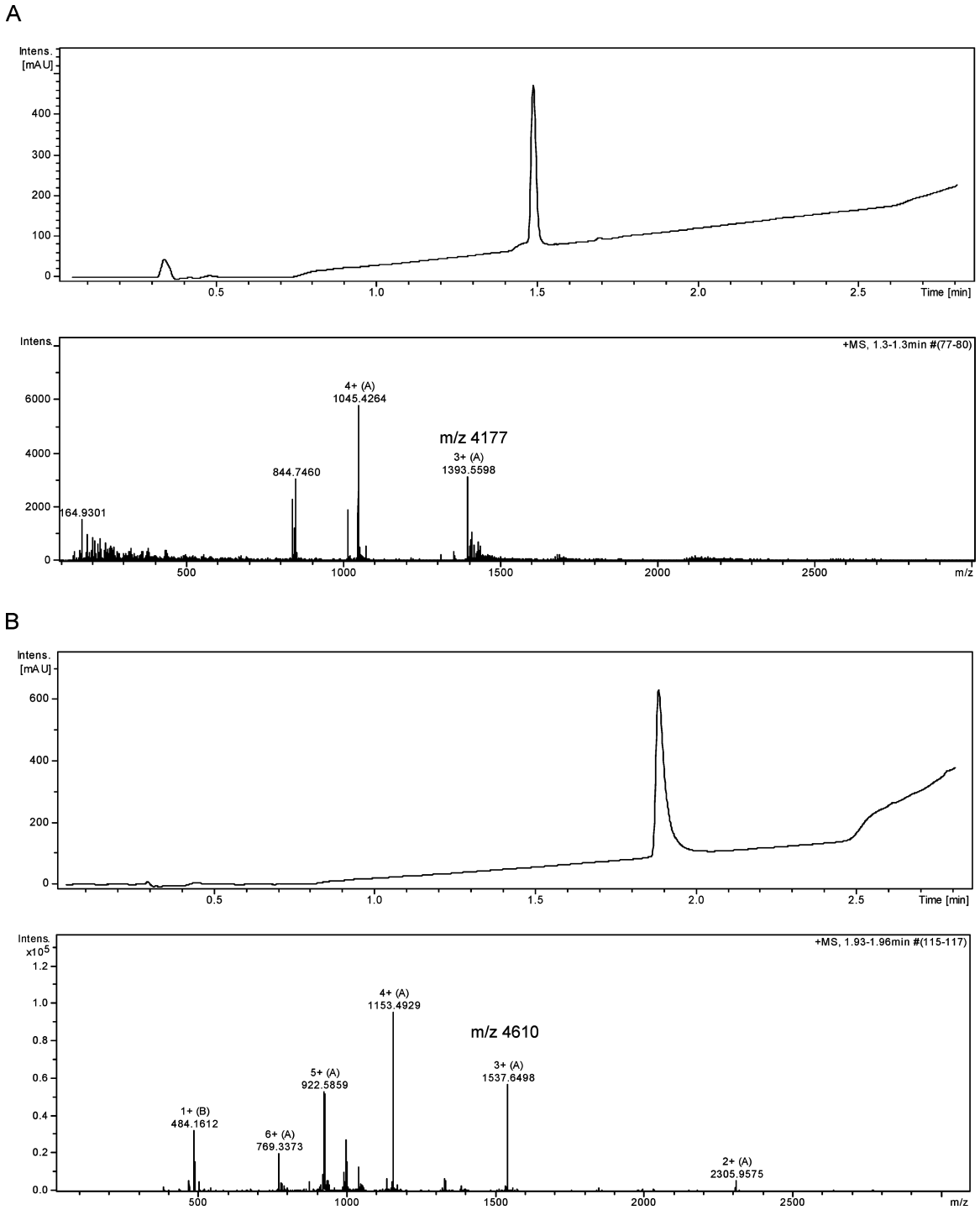

Figure 3. LC-MS analysis of **2**, and **3**. (A) Representative mass spectrum of **2** with monitoring at $m/z = 4178$. (B) Representative mass spectrum of **3** with monitoring at $m/z = 4610$.

or etoposide by HPLC or LC/MS analysis. On the basis of these results, the estimated half-lives for **2** and **3** were 24 and 63 min, respectively.

Cell Cycle Effects. Doxorubicin and etoposide arrest cells in the G2 phase of the cell cycle,[20,21] although the mechanism may be different for both agents.[22,23] The cytotoxic effect of doxorubicin on malignant cells is thought to be related to nucleotide base intercalation and cell membrane lipid binding. DNA intercalation of doxorubicin inhibits the action of DNA and RNA polymerases and interacts with topoisomerase II to form DNA-cleavable complexes, resulting ultimately in a cell-cycle pause in G2. The role of cellular membrane binding in this process remains unclear. Etoposide is thought to produce breaks by either interacting directly with topoisomerase II or by participating in the formation of free radicals, which again pauses cells in G2. To analyze whether **2** and **3** had similar cell cycle effects, U87 MG glioblastoma cells were treated with **2** (33 nM), doxorubicin (100 nM), **3** (1 μM), or etoposide (3 μM) for 48 h and cellular DNA content was determined by flow cytometry (Table 3).

In the experiments comparing doxorubicin to **2**, cells prior to drug addition were distributed across the cell cycle in a

Table 2. In Vitro Cytotoxicity of **2** and **3**[a]

	IC_{50} (nM)		
	glioblastoma (U87 MG)	hepatocarcinoma (SK-Hep-1)	lung carcinoma (NCI-H460)
2	6.0	4.6	7.3
doxorubicin	18	10	11
3	330	48	148
etoposide	145	62	90

[a] Values are means of 3−5 experiments ($n = 8$).

Table 3. Effects of **2** and **3** on the Cell Cycle[a]

	cell cycle phase (%)		
molecules	G0/G1	S	G2/M
control	58.2	14.1	27
doxorubicin	30.8	8.9	59.9
2	32.3	10.1	57.3
control	56.8	5.1	38
etoposide	8.9	4.2	87
3	25.7	3.3	70.8

[a] U87 MG glioblastoma cells were treated for 24 h with no drug (control), doxorubicin, 100 nM, or product **2**, 33 nM. U87 glioblastoma cells were also treated for 24 h with no drug (control), etoposide, 3 μM, and product **3**, 1 μM. DNA cellular content was analyzed by flow cytometry. Results are presented as the percentage of cells in each cell cycle phase. One representative experiment of three is shown.

normal logarithmic growth pattern, with 27% of the cells in the G2/M phase of the cell cycle (Table 3). Addition of doxorubicin increased the proportion of cells in G2/M to 59.9%, as expected from earlier published reports. Addition of the Angiopep-2-doxorubicin derivative **2** also increased the percentage of cells in G2/M to nearly the same extent, 57.3%, as unconjugated doxorubicin. Similarly, the proportion of cells in G2/M rose from 38% in drug-naïve cells to 87% and 70.8% after treatment with etoposide and the Angiopep-2-etoposide derivative **3**, respectively. Thus, treatment with doxorubicin and **2**, as well as etoposide and **3**, produced very similar cell cycle delays in G2/M, consistent with the conjugated and unconjugated drugs having similar molecular effects.

Blood−Brain Barrier Influx Rate Constants. We used an in situ brain perfusion method,[24,25] previously adapted in our laboratory,[15] to measure the transport of **2** and **3** into brain tissue in mice (Experimental Section). In brief, [^{125}I]-**2**, [^{14}C]-doxorubicin, [^{125}I]-**3**, or [^{3}H]-etoposide were perfused in situ into the carotid artery for 0.5, 1, 2, or 4 min, followed by a tracer-free washout period of 60 s. After perfusion, the animals were sacrificed, the brain was surgically removed and homogenized, and radioactivity in total brain tissue was quantified. In the total brain homogenate, V_d increased in a linear fashion for **2** (Figure 4A) and **3** (Figure 5A), exhibiting no evidence of saturation after 4 min of perfusion for either agent. By comparison, the V_d values for doxorubicin and etoposide were low and remained relatively constant over the same period, indicating little uptake of unconjugated drugs into total brain tissue. The slopes of the curves, which correspond to the BBB influx rate constants (K_{in}), are presented in Table 4. The K_{in} for **2** ($31 \pm 0.7 \times 10^{-4}$ mL/g/s) was 12.4-fold greater than unconjugated doxorubicin ($2.5 \pm 0.1 \times 10^{-4}$ mL/g/s), while the K_{in} for **3** ($22 \pm 0.2 \times 10^{-4}$ mL/g/s) was 24.4-fold greater than unconjugated etoposide ($0.9 \pm 0.1 \times 10^{-4}$ mL/g/s). Thus, both new Angiopep-2 drug conjugates exhibited dramatically higher BBB influx rate constants than their unconjugated precursors, consistent with an enhanced ability to cross the BBB. The observed K_{in} values for **2** and **3** were similar to **1** ($33 \pm 0.2 \times 10^{-4}$ mL/g/s) (Table 3), suggesting similar influx kinetics for the three drugs. In control experiments, [^{14}C]-inulin, which is normally excluded from brain tissue in vivo, was perfused in the presence of unlabeled **2** and **3** to verify the physical integrity of the BBB (data not shown).

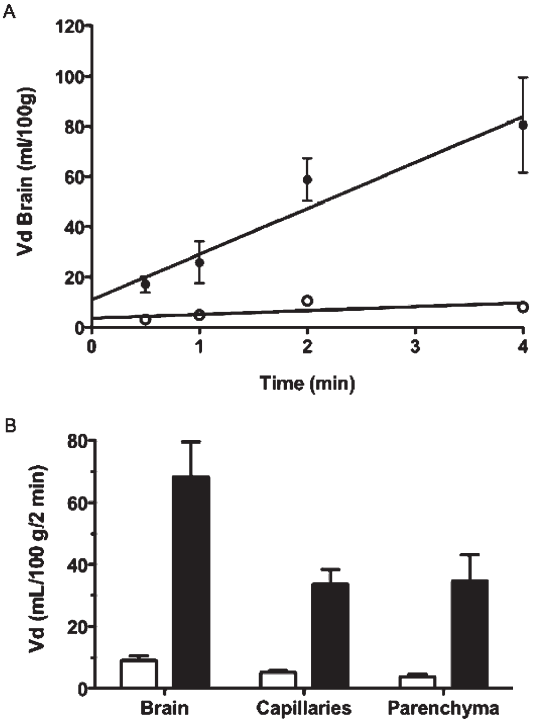

Figure 4. In vivo brain uptake of **2**. (A) Time course of brain uptake of [^{125}I]-**2** (filled circles) and [^{14}C]-doxorubicin (open circles) measured by in situ brain perfusion. Results were expressed as the apparent volume of distribution (V_d) for the radiolabeled **2** or doxorubicin in total brain homogenate. Lines represent best fits to the data by least-squares regression. (B) After a 2 min perfusion of [^{125}I]-**2** (filled bars) and [^{14}C]-doxorubicin (open bars), brain capillary depletion was performed and radioactivity was quantified in total brain homogenate, brain capillary fractions, and brain parenchymal fractions (Experimental Section). Results were expressed as the apparent volume of distribution (V_d) for the radiolabeled drugs found in these brain compartments. All data represent mean ± SD ($n = 3-6$ per time point).

Parenchymal Uptake. To formally analyze whether **2** and **3** enter brain parenchyma or remain associated with the brain capillary endothelium, we estimated the apparent volume of distribution (V_d) for the two agents in total brain tissue, brain capillaries, and brain parenchyma after in situ perfusion and brain capillary depletion. For the brain capillary depletion, the brain was collected and homogenized as described above and then subjected to differential centrifugation through 35% Dextran 70.[15] The radioactivity was then quantified in the capillary (pellet) and parenchymal (supernatant) fractions. At the 2 min time point, both **2** (Figure 4B) and **3** (Figure 5B) were present in parenchymal tissue at levels significantly higher than unconjugated doxorubicin and etoposide, indicating a higher rate of passage across the BBB for both agents relative to their parental precursors. By comparison, the V_d values for doxorubicin and etoposide were low and remained relatively constant over the same period, indicating little uptake of parental drugs into parenchymal tissue or total brain tissue. Significant

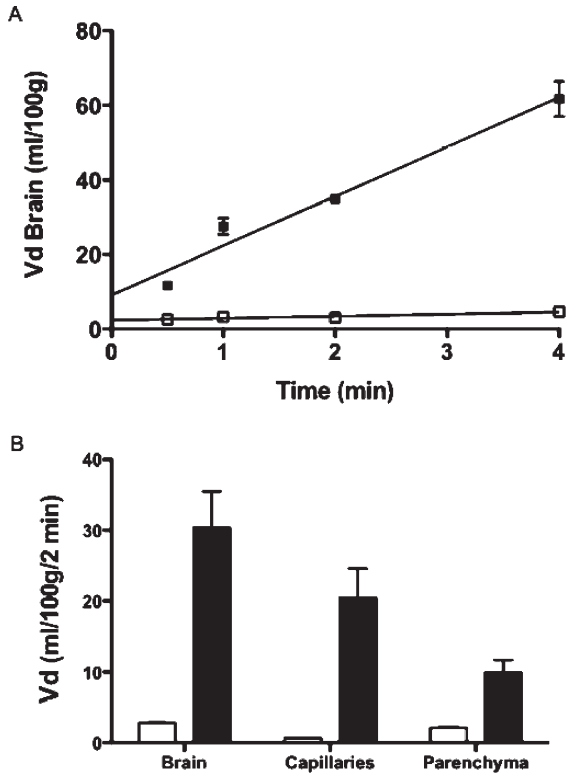

Figure 5. In vivo brain uptake of **3**. (A) Time course of brain uptake of [^{125}I]-**3** (filled circles) and [^{3}H]-etoposide (open circles) measured by in situ brain perfusion. Results were expressed as the apparent volume of distribution (V_d) for the radiolabeled **3** or etoposide in total brain homogenate. Lines represent best fits to the data by least-squares regression. (B) After a 2 min perfusion of [^{125}I]-**3** (filled bars) and [^{3}H]-etoposide (open bars), brain capillary depletion was performed and radioactivity was quantified in total brain homogenate, brain capillary fractions, and brain parenchymal fractions (Experimental Section). Results were expressed as the apparent volume of distribution (V_d) for the radiolabeled drugs found in these brain compartments. All data represent mean ± SD (n = 3−6 per time point).

Table 4. Blood−Brain Barrier Influx Rate Constants for New Angiopep-2 Modified Anticancer Drugs and Their Respective Unmodified Analogues

	brain K_{in} ($\times 10^{-4}$ mL/g/s)
2	31 ± 0.7
doxorubicin	2.5 ± 0.1
3	22 ± 0.2
etoposide	0.9 ± 0.1
1	33 ± 0.2
pacitaxel	6.9 ± 0.5

levels of **2** and **3** were also observed in the capillary fraction, as expected from the extraordinarily high density of brain capillaries.[26]

Transport of 2 and 3 in *Mdr1a* (−/−) mice. Brain capillary endothelial cells contain multiple efflux pumps that protect the brain from unwanted chemical assaults and contribute to the intrinsic or acquired multidrug resistance (MDR) that can arise after prolonged chemotherapy.[27−29] In humans, one of the most important efflux pumps expressed at the BBB is the ATP-binding cassette (ABC) transporter protein B1 (ABCB1) also known as MDR1 or P-glycoprotein (P-gp). At the BBB, this efflux pump limits the entry to the brain of a vast array of anticancer agents, including doxorubicin and etoposide.[30,31]

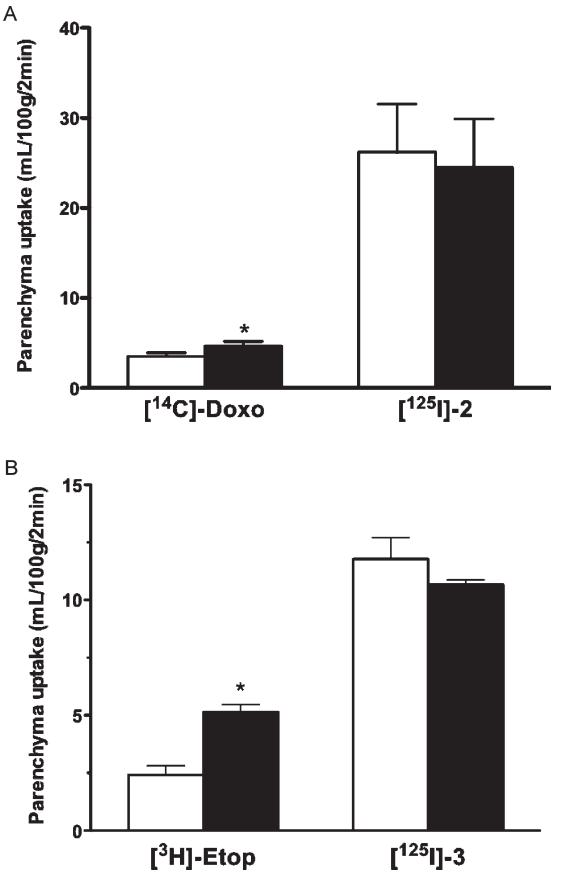

Figure 6. In situ brain perfusion in wild-type and *Mdr-1a* (−/−) knockout mice. Brain parenchyma uptake of (A) [^{125}I]-**2** and [^{14}C]-doxorubicin (B) [^{125}I]-**3** and [^{3}H]-etoposide measured by in situ brain perfusion in wild-type (open bars) and *Mdr1a* (−/−) mice (closed bars). Mice were perfused with 250 nM of [^{125}I]-**2**, 750 nM [^{14}C]-doxorubicin, 250 nM of [^{125}I]-**3**, or 250 nM [^{3}H]-etoposide for 2 min prior to brain capillary depletion and quantification of radioactivity (Experimental Section). Results are expressed as the apparent volume of distribution (V_d) for the radiolabeled drugs found in the brain parenchyma. Data represent the means ± SD obtained for at least three mice. *P = 0.023, *Mdr1a* (−/−) mice vs wild type in the doxorubicin-treated animals.

In mice, ABCB1 is encoded by three *Mdr* genes,[32−35] and previous studies have demonstrated that the *Mdr1a* isoform is expressed at the BBB in mice.[36]

The role of ABCB1 in the BBB can be conveniently assayed using *Mdr1a* (−/−) mice, which lack this transporter and consequently exhibit greater brain accumulation of many peripherally administered drugs.[36−38] Consistent with the demonstrated role of this pump in the efflux of doxorubicin and etoposide at the BBB, mice bearing homozygous mutations of *Mdr1a* exhibited >1.3- and 2-fold increased brain penetration of unconjugated doxorubicin (Figure 6A) and etoposide (Figure 6B) relative to wild type control mice, respectively. These increases in doxorubicin and etoposide brain uptake are similar to previous published data.[25] By comparison, brain parenchymal uptake was similar in the wild type and mutant mice for both **2** and **3**, indicating that they are not substrates for ABCB1 at the BBB. Furthermore, the brain penetration of both **2** and **3** was much higher in the *Mdr1a* (−/−) knockout mice than their parental drugs, suggesting that other efflux pumps could limit the entry of the unconjugated drugs into brain tissue. One candidate could be the breast cancer resistance

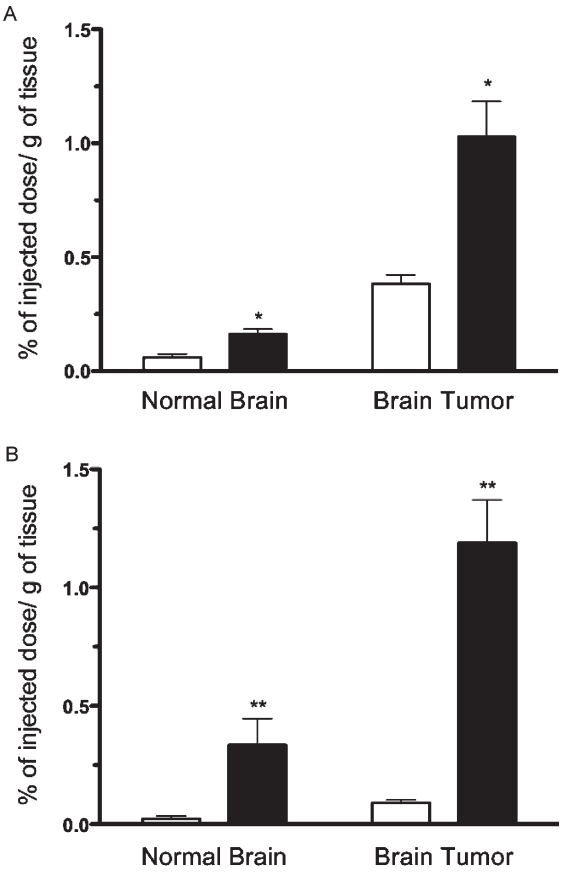

Figure 7. Tissue distribution in mouse brain with U87 glioma tumors. Brain biodistribution after intravenous bolus injection of (A) [^{125}I]-**2** (filled bars) and [^{14}C]-doxorubicin (open bars) and (B) [^{125}I]-**3** (filled bars) and [^{3}H]-etoposide (open bars) measured in normal brain and brain tumors. Mice were injected with 15 mg/kg of [^{125}I]-**2**, 6 mg/kg [^{14}C]-doxorubicin, 20 mg/kg of [^{125}I]-**3**, or 8 mg/kg [^{3}H]-etoposide. Thirty min after injection, mice were perfused by the heart, brain tissues were dissected and weighed, and radioactivity in the brain tumor (implanted hemisphere) and normal brain tissue (contralateral hemisphere) was quantified (Experimental Section). Results are expressed as the % of injected dose per gram of tissue. Data represent the means ± SD obtained for three mice (*$P < 0.05$, ** $P < 0.01$).

protein (BCRP or ABCG2), which is also expressed at the BBB in rodents.[14] Both doxorubicin and etoposide have been reported to be substrates for BCRP.[39,40] Overall, the preceding results indicate that drugs and other substrates of the ABCB1 efflux pump at the BBB may be modified with Angiopep-2 to produce derivatives with enhanced brain uptake.

Increased Brain Tissue Distribution. Finally, we measured the accumulation of **2** and **3** in an orthotopic mouse brain tumor model (Figure 7). Substantial differences were observed in the biodistribution patterns of the two conjugates compared to their parental drugs (doxorubicin and etoposide). For both **2** and **3**, penetration into normal brain tissue and tumor tissue after an intravenous bolus injection was significantly higher than the parental drugs. When the percentage of injected dose of drug per gram of tissue was calculated, penetration of **2** increased by 3-fold in normal brain tissue and by 2-fold in brain tumor tissue compared to doxorubicin. By comparison, penetration of **3** increased by 15-fold in normal brain tissue and by 13-fold in tumor tissue compared to etoposide.

The results presented here and in previous publications[13,15,16,41] lay the groundwork for assessing the potential of the EPiC platform in neurotherapeutic development. Several key features of the technology have now been documented. First, NCEs developed to date using Angiopep-2 have all exhibited highly efficient transport across the BBB. Thus **2**, **3**, and **1** each had significantly higher BBB K_{in} values than doxorubicin, etoposide, and paclitaxel, respectively. Moreover, the K_{in} values for all three agents compared favorably to glucose (63×10^{-4} mL/g/s in rats),[42] which crosses the BBB by a specific carrier-mediated mechanism; morphine (1.6×10^{-4} mL/g/s in rats),[43] which crosses the BBB by nonspecific diffusion; and receptor-associated protein (1.0×10^{-4} mL/g/s),[44] which crosses the BBB by LRP-1 receptor-mediated transcytosis. Moreover, it is noteworthy that **2** and **3** both penetrated well into tumor tissue, encouraging further development of these agents as therapies for brain cancers.

Second, the tolerance of the Angiopep-2 peptide to chemical modification appears to be flexible. Angiopep-2 is a 19-amino-acid sequence derived from the Kunitz-type domain present on some LRP-1 ligands, such as aprotinin, bikunin, amyloid precursor protein, and tissue factor pathway inhibitor.[15] We now have evidence that **2**, **3**, and **1**, each of which carries three separate drug moieties, cross the BBB efficiently. The molecular mechanism explaining how these modifications to Angiopep-2 affect or modulate LRP-1 binding remains to be established. It should also be noted that doxorubicin, etoposide, and paclitaxel, although different in their chemical properties and hydrophilicities, are nonetheless relatively small. Currently, modification of Angiopep-2 with larger biologicals, including therapeutic peptides, monoclonal antibodies, and siRNA, is under investigation in our laboratory.[45]

Finally, no evidence to date would suggest that conjugation of the Angiopep-2 sequence to anticancer agents dramatically inhibits their activities. In this and earlier[16] studies, the in vitro cytotoxic activities of **2**, **3**, and **1** were similar to those of their unconjugated precursors, doxorubicin, etoposide, and paclitaxel, respectively. Moreover, **1** is currently in phase I clinical trials and has shown promising activity against primary and secondary brain cancers.[17,18] The prior data are consistent with our recent release studies, which indicate that the anticancer moieties are likely cleaved in vivo from Angiopep-2 conjugates prior to performing their antiproliferative activities. Again, the generality of these conclusions will require an analysis of more agents, including larger biologics, but preliminary evidence indicates that functionality may also remain after conjugation of neuroactive peptides, antibodies, and siRNAs to Angiopep-2.[45]

Conclusions

The identification of new neurotherapeutics that can cross the BBB has proven difficult in the past, and novel methodologies for enhancing cross-BBB transport have long been needed. The EPiC platform is based on a 19-amino-acid peptide (Angiopep-2) that shows high transport across brain capillary endothelial cells via an LRP1-mediated mechanism.[13,15,16,41] Using Angiopep-2, new chemical entities were created with enhanced transport across the BBB. The first agent developed with this platform was **1** , which carries three paclitaxel molecules conjugated to Angiopep-2. This study examined two new agents, **2** and **3**, which carry three molecules of doxorubicin and etoposide, respectively, conjugated

to Angiopep-2. Both agents killed cancer cell lines in vitro with similar IC_{50} values and with apparently similar cytotoxic mechanisms as unconjugated doxorubicin and etoposide. **2** and **3** also exhibited dramatically higher BBB influx rate constants than unconjugated doxorubicin and etoposide and pooled within brain parenchymal and tumor tissue. Passage through the BBB for both agents was not increased in mice lacking the ABCB1 efflux pump, implying their transport bypasses this pump system, which distinguishes the new agents from unconjugated doxorubicin and etoposide. In total, these results provide evidence that the novel drug development platform described here can be used broadly to isolate a range of small-molecule neurotherapeutics with increased brain penetration.

Experimental Section

Reagents. Doxorubicin hydrochloride and etoposide were purchased from Enzo Life Sciences (Plymouth Meeting, PA). All other reagents and anhydrous solvents were purchased from Sigma-Aldrich (St. Louis, MO) and used as received. NMR (^{1}H, ^{13}C) spectra were recorded on Varian AS600 spectrometers (Palo Alto, CA) in $CDCl_3$, CD_3OD, or DMSO with solvent resonance as the internal standard. Low- and high-resolution mass spectra were recorded on Bruker micrOTOF spectrometers (Billerica, MA) using electron spray ionization (ESI-TOF). The purity of the conjugate target compounds was determined to be >95% by UPLC/MS on a Waters Acquity UPLC spectrometer (Milford MA) and by HPLC on a Shimadzu SCL-10A HPLC (Columbia, MD). UPLC was conducted on an Acquity UPLC BEH phenyl 1.7 μm column (2.1 mm × 50 mm) using a gradient of 10−90% MeCN−water (0.1% FA) at 0.5 mL/min. HPLC was conducted on a Taxsil column 3 μm (4.6 mm × 50 mm) using a gradient of 10−70% MeCN−water (0.05% TFA) at 1 mL/min. Analytical thin-layer chromatography was performed on Merck 60F 254 precoated silica gel plates. Flash column chromatography was performed on a Biotage system (Charlottesville, VA) using Silicycle siliaflash cartridges (230−400 mesh). Purifications were performed with a 30 RPC column on an AKTAexplorer 100 instrument (GE Healthcare, Baie d'Urfé, QC, Canada).

Animals. All animals were handled and maintained in accordance with the Guidelines of the Canadian Council on Animal Care.[46] Animal protocols were approved by the Institutional Animal Care and Use Committee of Université du Québec à Montréal. Animals were obtained from Charles River Laboratories Inc. (Saint-Constant, QC, Canada) and were allowed to acclimatize for 5 days before experiments. Brain perfusion studies were performed on adult male Crl: CD-1 mice (25−30 g, 6−8 weeks old) (Charles River Canada, St-Constant, QC, Canada) and adult female CF-1 mice (*Mdr1a* (+/+) and (−/−), 30−40 g, 6−8 weeks old) (Charles River Inc., Wilmington, MA).

***N*-Fmoc Doxorubicin (4).** DIEA (1.5 mL, 8.63 mmol) was added dropwise to a solution of doxorubicin (2.0 g, 3.45 mmol) and FmocOSu (2.32 g, 6.9 mmol) in DMF (35 mL) under stirring. The mixture was stirred at room temperature for 2 h and concentrated. The resulting residue was triturated with 0.1% TFA in H_2O (3 × 20 mL) and washed with Et_2O (5 × 20 mL). The resulting red solid was collected and repurified using a Silicycle siliaflash 120 g cartridge on a Biotage system (2% to 10% MeOH in DCM) to give **4** as a red powder 2.1 g, 80%. UPLC purity was 98%. ^{1}H NMR (600 MHz, $CDCl_3$) δ (ppm) 7.96 (m, 1H), 7.72 (m, 2H), 7.56 (m, 1H), 7.36 (m, 2H), 7.29 (m, 2H), 7.06 (m, 2H), 5.45 (m, 1H), 5.24 (m, 2H), 4.76 (m, 2H), 4.35 (m, 1H), 4.16 (m, 2H), 4.06 (s, 3H), 3.8 (m, 2H), 3.62 (m, 1H), 3.23 (d, 1H, J = 17.7 Hz), 2.35 (m, 1H), 2.16 (m, 1H), 1.8 (m, 1H), 1.31 (d, J = 6.2 Hz, 3H). ^{13}C NMR (150 MHz, $CDCl_3$) δ (ppm) 215.0, 187.53, 187.04, 163.16, 161.58, 156.48, 156.15, 155.85, 144.41, 141.85, 136.46, 135.95, 135.60, 133.95, 128.27, 127.61, 125.58, 121.11, 120.50, 120.38, 119.02, 112.08, 111.76, 77.0, 69.85, 67.18, 66.14, 62.64, 57.25, 47.48, 37.11, 36.15, 34.41, 32.07, 17.36. LC-HRMS (ESI, MicrOTOF), m/z calcd for $C_{42}H_{39}NO_{13}$ 765.2421, found 788.2425 (M + Na).

***N*-Fmoc Doxorubicin Hemisuccinate (5).** DIEA (0.17 mL, 1.0 mmol) was added dropwise to a solution of *N*-Fmoc doxorubicin **4** (0.28 g, 0.366 mmol) and succinic anhydride (0.11 g, 1.1 mmol) in DMF (20 mL) under stirring. The mixture was stirred at room temperature and monitored by UPLC. After two days, the reaction did not progress any more. The solvent was removed, and the resulting residue was purified using Silicycle siliaflash 40 g cartridge on Biotage system (2% to 15% MeOH in DCM) to give **5** as a red powder 100 mg, 33%. UPLC purity, 95%. ^{1}H NMR (600 MHz, $CDCl_3$) δ (ppm) 7.96 (m, 1H), 7.74 (m, 2H), 7.56 (m, 2H), 7.36 (m, 2H), 7.29 (m, 2H), 7.06 (m, 2H), 5.45 (m, 1H), 5.35 (m, 2H), 5.2 (m, 2H), 4.35 (m, 1H), 4.18 (m, 2H), 4.05 (s, 3H), 3.8 (m, 2H), 3.6 (m, 1H), 3.23 (m, 1H), 2.95 (m, 1H), 2.79 (t, 2H, J = 7.0 Hz), 2.71 (t, 2H, J = 7.0 Hz), 1.98−2.2 (m, 4H), 1.23 (d, J = 6.3 Hz, 3H). ^{13}C NMR (150 MHz, $CDCl_3$) δ (ppm) 207.75, 187.63, 187.15, 175.07, 172.59, 172.49, 161.55, 156.34, 155.56, 144.42, 141.88, 136.40, 135.65, 133.97, 128.24, 128.23, 127.60, 125.60, 121.23, 120.49, 120.36, 118.99, 112.13, 111.78, 101.18, 98.54, 70.32, 69.99, 67.93, 66.95, 66.32, 62.48, 57.21, 47.81, 36.0, 33.94, 30.89, 30.66, 29.46, 29.35, 29.27, 17.26. LC-HRMS (ESI, MicrOTOF), m/z calcd for $C_{46}H_{43}NO_{16}$ 865.2582, found 888.2710 (M + Na).

Synthesis of 2. DIEA (0.25 mL, 1.44 mmol) was added dropwise to a solution of **5** (599 mg, 0.692 mmol) and TBTU (231 mg, 0.72 mmol) in DMF (21 mL) under stirring. The mixture was stirred at room temperature for 50 min, thus a solution of Angiopep-2 (671 mg, 0.229 mmol) in DMSO (2 mL) and DMF (12 mL) was added. The mixture was stirred at room temperature for 20 min. HPLC showed the reaction was complete. After stirring for another 10 min, the solvent was removed. The residue was purified using Biotage SNAP cartridge KP-C18-HS 120 g (40% to 80% MeCN in water with 0.05% TFA) to give Fmoc protected conjugate as a red powder 500 mg, UPLC purity, 95%. To a solution of above Fmoc protected conjugate (260 mg, 0.053 mmol) in DMSO (1 mL) and DMF (12 mL) was added piperidine (20% in DMF, 1.5 mL). The solution became blue. After stirring for 10 min, the solution was cooled to 0 °C and treated with FA (0.5 M in DMF, 6 mL) to get a clear red solution. The solvent was removed under reduced pressure. The resulting residue was triturated with Et_2O (3 × 10 mL) and EtOAc (3 × 10 mL). The resulting red solid was purified using 30 RPC column on AKTAexplorer (10−40% MeCN in water and 0.15% FA) to give **2** as a red powder 82 mg, 17% in two steps. UPLC purity, 95%. LC-HRMS (ESI, micrOTOF), m/z, calcd for $C_{197}H_{242}N_{32}O_{70}$ 4177.6428, found 2089.9674 (2+), 1393.2419 (3+), 1045.4395 (4+).

Etoposide 4′-Dimethylglycine (6). A mixture of etoposide (235 mg, 0.4 mmol) and DMAP (73 mg, 0.6 mmol) in DMF (4 mL) was stirred at room temperature for 20 min, then *N,N*-dimethylacetyl chloride (96 mg, 0.52 mmol) was added in one pot under stirring. After 30 min, the reaction was complete according to HPLC. FA (1 M in DMF, 0.5 mL) was added, and the solvent was concentrated to 1 mL. The resulting solution was loaded to a 30 RPC column on AKTAexplorer for purification (gradient 10−30% MeCN in H_2O with 0.1% FA). After lyophilization, **6** (180 mg, 67%) was obtained as a colorless powder. ^{1}H NMR (600 Hz, CD_3OD) δ (ppm) 7.01 (1H, s), 6.56 (1H, s), 6.39 (2H, s), 5.98 (2H, d, J = 2.9 Hz), 5.05 (1H, d, J = 3.4 Hz), 4.77 (1H, q, J = 4.9 Hz), 4.68 (1H, d, J = 5.4 Hz), 4.66 (1H, d, J = 7.8 Hz), 4.46 (2H, s), 4.45 (1H, dd, J = 10.3, 8.8 Hz), 4.31 (1H, t, J = 8.0 Hz), 4.17 (1H, dd, J = 10.3, 4.9 Hz), 3.68 (6H, s), 3.56 (1H, q, J = 10 Hz), 3.54 (1H, t, J = 9.3 Hz), 3.52 (1H, dd, J = 14.2, 5.6 Hz), 3.32 (1H, m), 3.26 (1H, dd, J = 9.1, 4.1 Hz), 3.24 (1H, dd, J = 9.2, 5.4 Hz), 3.02 (6H, s), 2.96 (1H, m), 1.33 (3H, d, J = 4.9 Hz). ^{13}C NMR (150 Hz, CD_3OD) δ (ppm)

175.26, 168.68, 151.35, 148.49, 147.01, 139.39, 132.74, 129.6, 127.28, 110.65, 110.45, 108.02, 102.19, 102.02, 99.25, 80.78, 75.06, 73.39, 72.41, 68.43, 68.01, 66.44, 59.73, 56.63, 56.47, 45.03, 43.86, 37.89, 20.99. LC-HRMS (ESI, micrOTOF) calcd for $C_{33}H_{39}NO_{14}$ 673.2371, found 674.2534 (M + 1).

Etoposide 4′-Dimethylglycine 2″-Hemiglutarate (7). A mixture of **6** (655 mg, 0.97 mmol) and DMAP (18 mg, 0.15 mmol) in chloroform (11 mL) was cooled to 0 °C. DMF (3 mL) and DIEA (0.25 mL, 1.46 mmol) were added consecutively, followed by glutaric anhydride (222 mg, 1.94 mmol). The reaction mixture was stirred at room temperature, monitored by HPLC. After 2 days, the solvent was concentrated to 3 mL. The resulting solution was loaded to a 30 RPC column on AKTAexplorer for purification (gradient, 10−30% MeCN in H_2O). After lyophilization, **7** (305 mg, 40%) and **8** (38 mg, 5%) were obtained as a white powder. **7**, ^{1}H NMR (600 Hz, CD_3OD) δ (ppm) 7.0 (1H, s), 6.53 (1H, s), 6.39 (2H, s), 5.99 (2H, d, J = 4.6 Hz), 4.97 (1H, q, J = 7.9 Hz), 4.94 (1H, d, J = 3.2 Hz), 4.78 (1H, q, J = 4.75 Hz), 4.74 (1H-2″, dd, J = 9.2, 8.0 Hz), 4.68 (1H, d, J = 5.6 Hz), 4.45 (2H, s), 4.41 (1H, dd, J = 9.6, 8.8 Hz), 4.29 (1H, t. J = 8.2 Hz), 4.15 (1H, dd, J = 10.0, 4.5 Hz), 3.78 (1H-3″, t, J = 9.4 Hz), 3.69 (6H, s), 3.61 (1H, t, J = 10.2 Hz), 3.42 (1H, td, J = 9.6, 5.2 Hz), 3.33 (1H, dd, J = 8.7, 8.2 Hz), 3.3 (1H, dd, J = 13.4, 5.3 Hz), 3.02 (6H, s), 2.93 (1H, m), 2.26 (1H, m), 2.16 (2H, m), 2.02 (1H, m), 1.64 (2H, m), 1.32 (3H, d, J = 4.9 Hz). ^{13}C NMR (150 Hz, CD_3OD) δ (ppm) 175.96, 175.33, 172.46, 163.74, 151.14, 148.96, 147.43, 139.53, 131.90, 129.83, 126.42, 110.20, 109.18, 107.40, 101.91, 100.65, 99.63, 80.39, 74.55, 73.95, 71.55, 71.29, 68.43, 67.82, 66.46, 56.43, 55.35, 43.90, 43.15, 40.82, 38.0, 32.86, 32.59, 19.93, 19.39. HRMS (ESI, MicrOTOF) calcd for $C_{38}H_{45}NO_{17}$ 787.2687, found 788.2432 (M + 1). Etoposide 4′-dimethylglycine 3″-hemiglutarate (**8**), ^{1}H NMR (600 Hz, CD_3OD) δ (ppm) 7.0 (1H, s), 6.54 (1H, s), 6.38 (2H, s), 5.98 (2H, q, J = 4.0 Hz), 5.09 (1H, t, J = 9.2 Hz), 5.05 (1H, d, J = 3.2 Hz), 4.76 (1H-3″, d, J = 7.6 Hz), 4.73 (1H, q, J = 5.1 Hz), 4.66 (1H, d, J = 5.6 Hz), 4.44 (1H, dd, J = 10.5, 8.8 Hz), 4.30 (1H, t. J = 8.0 Hz), 4.18 (1H, dd, J = 10.3, 4.5 Hz), 3.67 (6H, s), 3.58 (2H, s), 3.57 (m, 1H), 3.48 (1H, dd, J = 14.0, 5.5 Hz), 3.44 (1H-2″, t, J = 10.2 Hz), 3.43 (1H, t, J = 9.4 Hz), 3.41 (1H, dd, J = 9.4, 4.1 Hz), 2.98 (1H, m), 2.47 (6H, s), 2.43 (2H, t, J = 7.0 Hz), 2.35 (2H, t, J = 7.4 Hz), 1.64 (2H, m), 1.32 (3H, d, J = 4.9 Hz). ^{13}C NMR (150 Hz, CD_3OD) δ (ppm) 176.27, 173.01, 167.79, 151.43, 148.94, 147.38, 139.21, 132.40, 129.21, 109.96, 109.78, 107.48, 102.28, 101.76, 99.53, 78.38, 73.75, 73.19, 72.64, 68.57, 67.87, 66.30, 58.81, 55.29, 44.06, 43.93, 40.98, 38.08, 33.16, 32.85, 20.49, 19.35. HRMS (ESI, MicrOTOF) calcd for $C_{38}H_{45}NO_{17}$ 787.2687, found 788.2432 (M + 1).

Synthesis of 3. DIEA (0.17 mL, 0.98 mmol) was added dropwise to a mixture of **7** (330 mg, 0.42 mmol) and TBTU (145 mg, 0.46 mmol) in DMF (24 mL). The mixture was stirred at room temperature for 50 min, then a solution of Angpep-2 (422 mg, 0.14 mmol) in DMSO (1.5 mL) and DMF (9 mL) was added, followed by DIEA (0.084 mL, 0.48 mmol). The mixture was stirred at room temperature for 20 min. An aliquot (10 μL) was taken for UPLC analysis, and it showed the reaction was complete. After stirring for another 10 min, the reaction solution was concentrated to 3 mL and purified using AKTA RPC column (gradient 10− 25% MeCN in H_2O with 0.05% FA). After lyophilization, **3** (172 mg, 26%) was yielded as a colorless powder. LC-HRMS (ESI, MicrOTOF), m/z calcd for $C_{218}H_{281}N_{32}O_{79}$ 4610.8955, found 2305.9327 (2+), 1537.6443 (3+), 1153.7463 (4+), 922.7970 (5+).

Iodination of 2 and 3 Derivatives. 2 and **3** were radiolabeled with standard procedures using an Iodo-beads kit. A ratio of two Iodo-beads per iodination was used for the labeling. Briefly, beads were washed twice with 1 mL of PBS on a Whatman filter and resuspended in 60 μL of PBS, pH 6.5. [^{125}I]Na (1 mCi) was added to the bead suspension for 5 min at room temperature. Iodination of peptide derived anticancer drugs was initiated by the addition of 250 μg of **2** or **3** (100−150 μL) diluted in 0.1 M PBS, pH 6.5. After incubation for 10 min at room temperature, Iodo-beads were removed and the supernatants were applied to a C18 column and purified by HPLC to remove free iodine. After iodination, radiolabeled products were reanalyzed by HPLC and results show that more than 95% of the radioactivity was associated to **2** or **3**.

In Vitro Cytotoxic Activity. For the thymidine uptake assay, tumor cells were cultured in 96-well plates at a density of 5000 cells per well. After incubation of cells with anticancer drugs for 48 h, the medium was aspirated and cells were pulse labeled for 2 h at 37 °C with a medium containing 2 μCi/mL [methyl-^{3}H]-thymidine (GE Healthcare). Cells were harvested and placed in a MicroBeta counter (1450 MicroBeta liquid scintillation and luminescence Counter; Perkin-Elmer) for determination of tritium uptake. Incorporated [^{3}H]-thymidine was plotted as a function of drug concentration. Concentration values required to get a 50% inhibition (IC50) were estimated using GraphPad software (La Jolla, CA).

In Vitro Half-Life Analysis. Stock solutions of **2** and **3** were prepared at 1 mg/mL in D5W (dextrose 5% in water). **2** and **3** at different concentrations (10−50 μg/mL) were incubated in human serum at 37 °C for 0 to 4 h. Serum proteins were precipitated by adding 370 μL of acetonitrile to 200 μL of serum, samples were vortexed and centrifuged, and the acetonitrile phases were transferred to clean glass tubes for LC/MS analysis.

In Vitro Cell Cycle Analysis Using Flow Cytometry. Exponential U87 MG cells growing in 25 cm^2 flasks were treated with equimolar concentrations of **2** (33 nM), doxorubicin (100 nM), **3** (1 μM), or etoposide (3 μM) for 48 h. After treatment, attached cells were released by trypsinization. Cells were centrifuged, washed twice with PBS, and fixed with 70% ice-cold ethanol. Fixed cells were resuspended in a DNA staining solution containing 50 μg/mL propidium iodide and 0.5 mg/mL RNase in 10 mM Tris and 5 mM $MgCl_2$. DNA cellular content was analyzed by fluorescence-activated cell sorting (FACS) on a FACS Calibur flow cytometer (Becton Dickinson, San Jose, CA) using CellQuest Pro software, version 4.0.2.

In Situ Mouse Brain Perfusion. The transport of [^{125}I]-**2**, [^{125}I]-**3**, and [^{14}C]-doxorubicin or [^{3}H]-etoposide in mouse brain was measured using the in situ brain perfusion method adapted in our laboratory for the study of drug uptake in the mouse brain (Dagenais et al.[24]). In situ brain perfusion of [^{14}C]-inulin in the presence of unlabeled **2** and **3** was also performed to verify the physical integrity of the BBB. Briefly, the right common carotid of mice anaesthetized with ketamine/xylazine (140/8 mg kg^{-1}, ip) was exposed and ligated at the level of the bifurcation of the common carotid, rostral to the occipital artery. The common carotid artery was then catheterized rostrally with polyethylene tubing filled with heparin (25 U/mL) and mounted on a 26-gauge needle. The syringe containing the perfusion fluid (radiolabeled molecules at the appropriate concentrations in Krebs/bicarbonate buffer (128 mM NaCl, 24 mM $NaHCO_3$, 4.2 mM KCl, 2.4 mM NaH_2PO_4, 1.5 mM $CaCl_2$, 0.9 mM $MgCl_2$ and 9 mM D-glucose) gassed with 95% O_2 and 5% CO_2 to obtain a pH of 7.4, and warmed to 37 °C in a water bath) was placed in an infusion pump (Harvard pump PHD 2000; Harvard Apparatus, Saint-Laurent, QC, Canada) and connected to the catheter. Prior to the perfusion, the contralateral blood flow contribution was eliminated by severing heart ventricles. The brain was perfused for 5 min at a flow rate of 1.15 mL/min. After perfusion, the brain was further perfused for 60 s with Krebs buffer to wash out the excess of radiolabeled molecules. Mice were then decapitated to terminate perfusion and the right hemisphere was quickly isolated on ice before being subjected to capillary depletion. Briefly, for capillary depletion, the mice brain was homogenized on ice in Ringer's HEPES buffer with 0.1% BSA in a glass homogenizer. Brain homogenate was then mixed thoroughly with 35% Dextran 70 (50:50) and centrifuged at 5400g for 10 min at 4 °C. The supernatant composed of brain parenchyma and the pellet

representing capillaries were then carefully separated. Aliquots of homogenates, supernatants, pellets, and perfusates were taken to measure their contents in radiolabeled molecules. Aliquots of the perfusion fluid were also collected and weighed to determine tracer concentrations in the perfusate. [^{125}I]-**2** and [^{125}I]-**3** samples were counted in a Wizard 1470 automatic γ counter (Perkin-Elmer Inc., Woodbridge, ON). [^{3}H]-Etoposide and [^{14}C]-doxorubicin samples were digested in 2 mL of Solvable (Packard) at 50 °C and mixed with 9 mL of Ultima gold XR scintillation cocktail (Packard). Radioactivity was counted in a Packard Tricarb model 1900 TR.

Brain Tissue Distribution. The tissue distribution of [^{125}I]-**2**, [^{125}I]-**3**, [^{14}C]-doxorubicin, or [^{3}H]-etoposide was measured in nu/nu mice bearing orthotopic U87 glioma tumors. Briefly, female athymic nude mice (Crl:Nu/Nu-*nu*BR; 20−25 g, 4−6 weeks old) (Charles River Canada, St. Constant, QC) were maintained in a pathogen-free environment. Intracerebral tumors were established by stereotactic inoculation of 5×10^5 U87 cells in mice brain as described.[16] Sixteen days after inoculation, when first presenting with significant body weight loss, the mice were used for the tissue distribution studies. [^{125}I]-**2** and [^{14}C]-doxorubicin were administered at doses of 15 and 6 mg/kg, respectively, by intravenous bolus injection. [^{125}I]-**3** and [^{3}H]-etoposide were also administered by intravenous bolus injection at doses of 20 and 8 mg/kg, respectively. Thirty min after injection, mice were anaesthetized with ketamine/xylazine (140/8 mg/kg, ip), whole blood was collected, and animals were then perfused by the heart with cold saline for 15 min at a flow rate of 5 mL/min. At the end of the perfusion, major organs were dissected and weighted. Brain hemispheres were separated, and the brain tumor mass was carefully dissected and weighed. The contralateral hemisphere served as the normal brain control. [^{125}I]**2** and [^{125}I]**3** tissue samples were counted in a Wizard 1470 automatic γ counter (Perkin-Elmer Inc., Woodbridge, ON). [^{3}H]-etoposide and [^{14}C]-doxorubicin tissue samples were digested in 2 mL of Solvable (Packard, Boston, MA) at 50 °C and mixed with 9 mL of Ultima gold XR scintillation cocktail (Packard, Boston, MA). Radioactivity was counted in a Packard Tri-Carb liquid scintillation counter model 1900 TR.

Acknowledgment. We thank Julie Poirier, Isabelle Lavallée, and Tran Nguyen for their technical support. This work was supported by research funding from the National Research Council of Canada's Industrial Research Assistance Program (NRC-IRAP) to Angiochem, Inc. and a grant from the Natural Sciences and Engineering Research Council of Canada (NSERC) to R. Béliveau. The authors also thank David Norris, PhD for editorial assistance provided during the preparation of this manuscript. This assistance was paid for through funding supplied by Angiochem, Inc. to Ecosse Medical Communications, LLC (Princeton, NJ). Disclosure: Angiochem, Inc., a biotechnology company located in Montreal, Canada, developed the EPiC drug platform described in this report. M.D. is an employee of Angiochem, Inc., has shares and stock options in the company, and is listed on company patent applications. C.C., G.Y., C.T., A.R., and J.-P.C. are employees, have stock options in the company, and are listed on company patent applications. M.-C.L. is also an employee and has stock options in the company. R.B. has received research funding and consulting fees from Angiochem, Inc., has shares in the company, and is listed on company patent applications. J.-C.C. reports no financial conflicts of interest pertaining to this work.

References

(1) Kleisbauer, J. P.; Vesco, D.; Orehek, J.; Blaive, B.; Clary, C.; Poirier, R.; Saretto, S.; Carles, P.; Dongay, G.; Guerin, J. C.; et al. Treatment of brain metastases of lung cancer with high doses of etoposide (VP16−213). Cooperative study from the Groupe Français Pneumo-Cancerologie. *Eur. J. Cancer Clin. Oncol.* **1988**, *24* (2), 131–135.

(2) Kobayashi, T.; Yoshida, J.; Ishiyama, J.; Noda, S.; Kito, A.; Kida, Y. Combination chemotherapy with cisplatin and etoposide for malignant intracranial germ-cell tumors. An experimental and clinical study. *J. Neurosurg.* **1989**, *70* (5), 676–681.

(3) Weiss, R. B. The anthracyclines: will we ever find a better doxorubicin? *Semin. Oncol.* **1992**, *19* (6), 670–686.

(4) Henderson, I. C.; Canellos, G. P. Cancer of the breast: the past decade (second of two parts). *N. Engl. J. Med.* **1980**, *302* (2), 78–90.

(5) Fornari, F. A.; Randolph, J. K.; Yalowich, J. C.; Ritke, M. K.; Gewirtz, D. A. Interference by doxorubicin with DNA unwinding in MCF-7 breast tumor cells. *Mol. Pharmacol.* **1994**, *45* (4), 649–656.

(6) Lee, J. S.; Murphy, W. K.; Glisson, B. S.; Dhingra, H. M.; Holoye, P. Y.; Hong, W. K. Primary chemotherapy of brain metastasis in small-cell lung cancer. *J. Clin. Oncol.* **1989**, *7* (7), 916–922.

(7) Baldwin, E. L.; Osheroff, N. Etoposide, topoisomerase II and cancer. *Curr. Med. Chem. Anticancer Agents* **2005**, *5* (4), 363–372.

(8) Bart, J.; Groen, H. J.; Hendrikse, N. H.; van der Graaf, W. T.; Vaalburg, W.; de Vries, E. G. The blood−brain barrier and oncology: new insights into function and modulation. *Cancer Treat. Rev.* **2000**, *26* (6), 449–462.

(9) Cecchelli, R.; Berezowski, V.; Lundquist, S.; Culot, M.; Renftel, M.; Dehouck, M. P.; Fenart, L. Modelling of the blood−brain barrier in drug discovery and development. *Nat. Rev. Drug. Discovery* **2007**, *6* (8), 650–661.

(10) Pardridge, W. M. Blood−brain barrier drug targeting: the future of brain drug development. *Mol. Interv.* **2003**, *3* (2), 90−105, 151.

(11) Pardridge, W. M. The blood−brain barrier: bottleneck in brain drug development. *NeuroRx* **2005**, *2* (1), 3–14.

(12) Pardridge, W. M. Drug targeting to the brain. *Pharm. Res.* **2007**, *24* (9), 1733–1744.

(13) Demeule, M.; Currie, J. C.; Bertrand, Y.; Che, C.; Nguyen, T.; Regina, A.; Gabathuler, R.; Castaigne, J. P.; Beliveau, R. Involvement of the low-density lipoprotein receptor-related protein in the transcytosis of the brain delivery vector angiopep-2. *J. Neurochem.* **2008**, *106* (4), 1534–1544.

(14) Loscher, W.; Potschka, H. Blood−brain barrier active efflux transporters: ATP-binding cassette gene family. *NeuroRx* **2005**, *2* (1), 86–98.

(15) Demeule, M.; Regina, A.; Che, C.; Poirier, J.; Nguyen, T.; Gabathuler, R.; Castaigne, J. P.; Beliveau, R. Identification and design of peptides as a new drug delivery system for the brain. *J. Pharmacol. Exp. Ther.* **2008**, *324* (3), 1064–1072.

(16) Regina, A.; Demeule, M.; Che, C.; Lavallee, I.; Poirier, J.; Gabathuler, R.; Beliveau, R.; Castaigne, J. P. Antitumour activity of ANG1005, a conjugate between paclitaxel and the new brain delivery vector Angiopep-2. *Br. J. Pharmacol.* **2008**, *155* (2), 185–197.

(17) Drappatz, J.; Brenner, A.; Rosenfeld, S.; Schiff, D.; Wen, P.; Mikkelsen, T.; Groves, M.; Wong, E. T.; Eichler, A.; Elian, K. M.; Lawrence, B.; Demeule, M.; Castaigne, J. P. ANG1005: Development of a new Engineered Peptide Compound (EPiC) for the Treatment of Malignant Glioma. Poster presented at: Neuroscience 2009, Chicago, IL, October 18, 2009.

(18) Kurzrock, R.; Gabrail, N.; Moulder, S.; Brenner, A.; Guo, Z.; Bouchard, D.; Churchill, W.; Bento, P.; Fitsialos, D.; Fraitag, B.; Neale, A.; Castaigne, J. P.; Sarantopoulos, J. ANG1005: A promising new Engineered Peptide Compound (EPiC) for Patients with Advanced Solid Tumors and Brain Metastases. Poster presented at: Neuroscience 2009, Chicago, IL, October 18, 2009.

(19) Zhang, K.; Franz, A.; Hill, G. C.; McCallum, C. M.; Minch, M. J. Etoposide: conformational and hydration features. *Magn. Reson. Chem.* **1999**, *37* (11), 788–798.

(20) Ling, Y. H.; el-Naggar, A. K.; Priebe, W.; Perez-Soler, R. Cell cycle-dependent cytotoxicity, G2/M phase arrest, and disruption of p34cdc2/cyclin B1 activity induced by doxorubicin in synchronized P388 cells. *Mol. Pharmacol.* **1996**, *49* (5), 832–841.

(21) Krishan, A.; Paika, K.; Frei, E., III. Cytofluorometric studies on the action of podophyllotoxin and epipodophyllotoxins (VM-26, VP-16-213) on the cell cycle traverse of human lymphoblasts. *J. Cell Biol.* **1975**, *66* (3), 521–530.

(22) *ETOPOPHOS—Etoposide Phosphate Injection, Powder, Lyophilized, for Solution* [package insert]; Bristol-Myers Squibb Company: Princeton, NJ, 2005.

(23) *Doxorubicin Hydrochloride for Injection* [package insert]; Pfizer Inc.: New York, 2006.

(24) Dagenais, C.; Rousselle, C.; Pollack, G. M.; Scherrmann, J. M. Development of an in situ mouse brain perfusion model and its

application to mdr1a P-glycoprotein-deficient mice. *J. Cereb. Blood Flow Metab*. **2000**, *20* (2), 381–386.
(25) Cisternino, S.; Rousselle, C.; Dagenais, C.; Scherrmann, J. M. Screening of multidrug-resistance sensitive drugs by in situ brain perfusion in P-glycoprotein-deficient mice. *Pharm. Res*. **2001**, *18* (2), 183–190.
(26) Duvernoy, H.; Delon, S.; Vannson, J. L. The vascularization of the human cerebellar cortex. *Brain Res. Bull*. **1983**, *11* (4), 419–480.
(27) Lage, H. An overview of cancer multidrug resistance: a still unsolved problem. *Cell. Mol. Life Sci*. **2008**, *65* (20), 3145–3167.
(28) Pauwels, E. K.; Erba, P.; Mariani, G.; Gomes, C. M. Multidrug resistance in cancer: its mechanism and its modulation. *Drug News Perspect*. **2007**, *20* (6), 371–377.
(29) Perez-Tomas, R. Multidrug resistance: retrospect and prospects in anti-cancer drug treatment. *Curr. Med. Chem*. **2006**, *13* (16), 1859–1876.
(30) Borst, P.; Elferink, R. O. Mammalian ABC transporters in health and disease. *Annu. Rev. Biochem*. **2002**, *71*, 537–592.
(31) Ambudkar, S. V.; Dey, S.; Hrycyna, C. A.; Ramachandra, M.; Pastan, I.; Gottesman, M. M. Biochemical, cellular, and pharmacological aspects of the multidrug transporter. *Annu. Rev. Pharmacol. Toxicol*. **1999**, *39*, 361–398.
(32) Devault, A.; Gros, P. Two members of the mouse mdr gene family confer multidrug resistance with overlapping but distinct drug specificities. *Mol. Cell. Biol*. **1990**, *10* (4), 1652–1663.
(33) Gros, P.; Croop, J.; Housman, D. Mammalian multidrug resistance gene: complete cDNA sequence indicates strong homology to bacterial transport proteins. *Cell* **1986**, *47* (3), 371–380.
(34) Gros, P.; Raymond, M.; Bell, J.; Housman, D. Cloning and characterization of a second member of the mouse mdr gene family. *Mol. Cell. Biol*. **1988**, *8* (7), 2770–2778.
(35) Raymond, M.; Gros, P. Mammalian multidrug-resistance gene: correlation of exon organization with structural domains and duplication of an ancestral gene. *Proc. Natl. Acad. Sci. U.S.A*. **1989**, *86* (17), 6488–6492.
(36) Schinkel, A. H. P-Glycoprotein, a gatekeeper in the blood−brain barrier. *Adv Drug Delivery Rev*. **1999**, *36* (2−3), 179–194.
(37) Schinkel, A. H.; Mayer, U.; Wagenaar, E.; Mol, C. A.; van Deemter, L.; Smit, J. J.; van der Valk, M. A.; Voordouw, A. C.; Spits, H.; van Tellingen, O.; Zijlmans, J. M.; Fibbe, W. E.; Borst, P. Normal viability and altered pharmacokinetics in mice lacking mdr1-type (drug-transporting) P-glycoproteins. *Proc. Natl. Acad. Sci. U.S.A*. **1997**, *94* (8), 4028–4033.
(38) Schinkel, A. H.; Smit, J. J.; van Tellingen, O.; Beijnen, J. H.; Wagenaar, E.; van Deemter, L.; Mol, C. A.; van der Valk, M. A.; Robanus-Maandag, E. C.; te Riele, H. P.; et al. Disruption of the mouse mdr1a P-glycoprotein gene leads to a deficiency in the blood−brain barrier and to increased sensitivity to drugs. *Cell* **1994**, *77* (4), 491–502.
(39) Doyle, L. A.; Ross, D. D. Multidrug resistance mediated by the breast cancer resistance protein BCRP (ABCG2). *Oncogene* **2003**, *22* (47), 7340–7358.
(40) Yuan, J.; Lv, H.; Peng, B.; Wang, C.; Yu, Y.; He, Z. Role of BCRP as a biomarker for predicting resistance to 5-fluorouracil in breast cancer. *Cancer Chemother. Pharmacol*. **2009**, *63* (6), 1103–1110.
(41) Thomas, F. C.; Taskar, K.; Rudraraju, V.; Goda, S.; Thorsheim, H. R.; Gaasch, J. A.; Mittapalli, R. K.; Palmieri, D.; Steeg, P. S.; Lockman, P. R.; Smith, Q. R. Uptake of ANG1005, a novel paclitaxel derivative, through the blood−brain barrier into brain and experimental brain metastases of breast cancer. *Pharm. Res*. **2009**, *26* (11), 2486–2494.
(42) Simpson, I. A.; Appel, N. M.; Hokari, M.; Oki, J.; Holman, G. D.; Maher, F.; Koehler-Stec, E. M.; Vannucci, S. J.; Smith, Q. R. Blood−brain barrier glucose transporter: effects of hypo- and hyperglycemia revisited. *J. Neurochem*. **1999**, *72* (1), 238–247.
(43) Seelbach, M. J.; Brooks, T. A.; Egleton, R. D.; Davis, T. P. Peripheral inflammatory hyperalgesia modulates morphine delivery to the brain: a role for P-glycoprotein. *J. Neurochem*. **2007**, *102* (5), 1677–1690.
(44) Pan, W.; Kastin, A. J.; Zankel, T. C.; van Kerkhof, P.; Terasaki, T.; Bu, G. Efficient transfer of receptor-associated protein (RAP) across the blood−brain barrier. *J. Cell Sci*. **2004**, *117* (Pt 21), 5071–5078.
(45) Gabathuler, R.; Demeule, M.; Regina, A.; Che, C.; Beliveau, R.; Castaigne, J. P. Development of a new Engineered Peptide Compound (EPiC) platform for the transport of small and large therapeutics to the CNS. Poster presented at: Neuroscience 2009, Chicago, IL, October 18, 2009.
(46) Canadian Council on Animal Care. Good animal practice in science; http://www.ccac.ca/ (Accessed July, **2009**).